DEVELOPMENT OF A PROTOTYPE OF A PROTECTIVE UV-C HALF-FACE MASK WITH IMPLEMENTATION OF ADDITIVE TECHNOLOGY

Daniel Varecha[1,*], Ján Galík[1], František Brumerčík[2], Róbert Kohár[2], Rudolf Madaj[2], Mário Drbúl[3], Adam Glowacz[4], Witold Glowacz[4], Hui Liu[5]

[1]Research and Service Centre, Faculty of Mechanical Engineering, University of Zilina, Zilina, Slovakia
[2]Department of Design and Mechanical Elements, Faculty of Mechanical Engineering, University of Zilina, Zilina, Slovakia
[3]Department of Machining and Production Technology, Faculty of Mechanical Engineering, University of Zilina, Zilina, Slovakia
[4]Department of Automatic Control and Robotics, Faculty of Electrical Engineering, Automatics, Computer Science and Biomedical Engineering, AGH University of Science and Technology, Krakow, Poland
[5]College of Quality and Safety Engineering, China Jiliang University, Hangzhou, China

*E-mail of corresponding author: daniel.varecha@fstroj.uniza.sk

Daniel Varecha 0000-0001-5894-407X,
František Brumerčík 0000-0001-7475-3724,
Rudolf Madaj 0000-0003-2458-2351,
Adam Glowacz 0000-0003-0546-7083,
Hui Liu 0000-0002-4265-7241
Ján Galík 0000-0003-4983-8851,
Róbert Kohár 0000-0001-7872-2829,
Mário Drbúl 0000-0002-8036-1927,
Witold Glowacz 0000-0002-8734-3844,

Resume

The authors of this manuscript present development of a prototype protective UV-C half-face mask. The first stage of this study focuses on proposing a UV-C half-face mask design and the second phase investigates the quality of printings, 3D/2D roughness and porousness of three different printed samples of PA12. Development of the protective half-face mask used the non-destructive technology of 3D scanning of the human body by the Ein Scan scanner. As a part of the experiment, three samples were prepared with Sinterit Lisa, EOS Formiga and HP jet fusion printers. SLS and MJF technology were used during the experiment. The experimental observation of the structure of the surface was secured using the Alicona Infinite focus G5 device. The conclusions present the study's results and the authors' recommendations for other developers dealing with the development of the protective face masks.

Article info

Received 16 February 2023
Accepted 20 March 2023
Online 29 March 2023

Keywords:

rapid prototyping
photogrammetry-3D projection
additive manufacturing, 2D/3D
roughness of PA12
selective laser sintering (SLS)
multi-jet fusion (MJF)

Available online: https://doi.org/10.26552/com.C.2023.038

ISSN 1335-4205 (print version)
ISSN 2585-7878 (online version)

1 Introduction

The human population has been susceptible to new respiratory diseases in the last two years. The emergence of COVID - 19 has sparked a worldwide demand for necessary measures to mitigate the spread of the infection [1]. At the end of 2019, hospitals reported a shortage of personal protective equipment for the frontline health workers [2]. Additive manufacturing brings a unique option to alleviated the lack of these critical medical aids [3]. At this time, the protective half-face masks are essential for masses of people to protect themselves and others from the virus's aerosol. Correct use of protective equipment significantly reduces the risk of virus transmission and protects the medical staff and other patients from infection [4]. It is a common knowledge that respiratory infections are caused mainly by different factors such as bacteria, fungi and viruses. This fact has been known for several tens of years. There are several ways to "fight" against these undesirable factors and keep your health in good condition. Among the primary and best-known methods are a healthy lifestyle, enough sleep, staying in the sun and a vitamin-rich diet. Vitamin D is important, which is essential in strengthening the human immune system [5]. The authors of the qualified manuscript [5] listed that

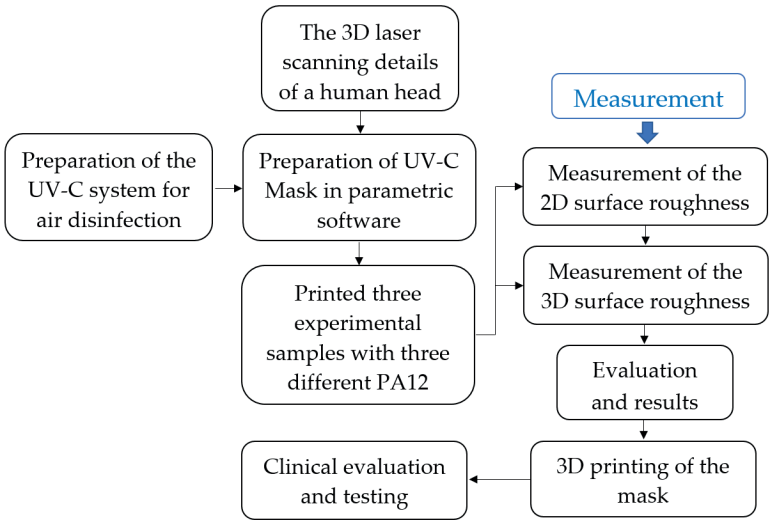

Figure 1 *Flowchart of the experimental setup*

vitamin D has a vital role in enhancing and increasing the immune system's ability. This characteristics of vitamin D prevents the virus's rapid spread in the lungs [5]. It also prohibits the penetration of viruses deep into tissues by maintaining intercellular connections [5]. These aspects contribute favorably to the correct functioning of the immune system, ultimately resulting in a good defense of the human body against these pathogens. However, after breaking through a weakened immune system, pathogens can cause respiratory disease. When an infection occurs, in most cases, medications must be started, which in the current 21st century is evident and effective in the fight against pathogens. Recently, increased number of people are discussing prevention, which is very important. In recent months, the public has used various surgical "no-name" face masks (products without company brand) to protect against respiratory diseases, which is not always quality protection. Wearing the protective face masks is utterly natural in Eastern culture (Asia). The population of Asia uses them not only to protect health but in the case of increased air chemical pollution (smog), as well.

The difference is the case in Europe and America, but the trend has changed and wearing a protective face mask has become a natural part of our lives in recent months. The authors of the manuscript [6] subjected surgical face masks to four simulated cycles of folding, aging with artificial saliva, or sweating and washing. They concluded that folding, saliva and sweat have little effect on the face mask's effectiveness and aging (depreciation). Research has confirmed that one can wear a worn surgical face mask longer than usual, the recommended four hours [6]. The pathogens have lived with us since time immemorial, so it is appropriate to introduce prevention and prevent infection.

The events from the last period have created a space for use of these technologies for disinfection, be it water, air, or surfaces with which a person comes into daily contact. For this reason, the authors of this manuscript began to develop a new type of the protective face mask that would disinfect the air with UV-C light. Value UV-C of the light is moving in the vast range from 100 to 280 nm and is used for disinfection increasingly in everyday life. Many researchers are currently working on the issue of UV-C light disinfection. When developing the protective face masks, information about the shape and features of the human head (face) is crucial. The imprint of the human face can be obtained only scientifically. Anthropology is a scientific field that focuses on measuring the external characteristics of the human body. Anthropology is necessary for developing and producing ergonomically correct workplaces or protective equipment.

Modern 3D scanners are also often used for this. Similar anthropological research took place in the U.S. in 2003 under the leadership of the National Institute for Occupational Safety and Health (NIOSH) [7] to update the respirator testing standards. The measurement was according to the traditional measure of anthropometric techniques on a sample of 3997 subjects, for 947 issues used, a Cyberware 3D Rapid Digitizer. Based on anthropometric data collected during the 2003 NIOSH survey, developed parameters at the National Personal Protective Technology Laboratory (NPPTL) for new digital models of the human head in five categories. The authors of [8] submitted the final report of this research in 2004. The digital head models from the NIOSH survey are symmetrical and represent the shape head-and-face distribution of current U.S. respirator users [9]. In the technical specification standard for protective equipment ISO TC94, upper respiratory protective equipment SC15, WG1 General and PG5 Human factors are also incorporated head forms [9]. The original journal National Library of Medicine [9] and several other highly qualified publications published the NIOSH anthropological data (2D and 3D). Many researchers during the COVID-19 crisis were dedicated to development of protective face masks.

An example can be a manuscript [10] in which authors present the custom-made face masks for pandemic crisis solutions, made using the 3D printing. In addition, the manuscript's authors [11] present a similar issue. The authors' study [12] examined the relationship between the definition of problems related to the COVID-19 pandemics and the characteristics of additive manufacturing solutions.

This study aims to design a protective UV-C half-mask and thus contribute to eliminating infection in society. At the beginning of the development of the protective half-face mask, the researchers established the following attributes as essential:

- The ideal shape designs;
- The high-quality non-porous material PA12;
- The surface structure of the half-face mask should not be enormously rough (the surface of the protective half-face mask will not need additional finishing after being printed out).

The flowchart (Figure1) shows the procedure for developing a prototype and the methods used to investigate the surface roughness of three different materials PA12.

2 Materials and methods

Additive technologies started to develop several decades ago and the development in a few years has grown exponentially. These developing additive technologies are significant and decisive for the fourth industrial revolution. Nowadays, increasing number of people come across devices that work on the principle of additive technologies. The use is very diverse and sometimes it is no longer possible to clearly say what was used in specific additive technology in production. Products realized by the additive technology also bring material and technical limitations that should be discussed more [13-14]. In the final process of the 3D printing, there may be limits, which can be manifested in the size of the printed object or the complex geometry. The current state of matters in the field of 3D printing does not allow fundamental structural changes in the standard design of a 3D printer [14]. The 3D printer forms a definite structure without the possibility of expanding individual parts of the device [14]. In addition, for this reason, a trend in the development of several researchers is a modular 3D printer, which solves these limitations and improves shortcomings. In the future, this would mean that after purchasing and asking for an increase in the construction area, only another block of, for example, the essential construction area would be needed [14]. The research and development details of the modular 3D printer are listed in [14].

In the past, most 3D printers, which worked on the principle of additive technology, used only one material during the printing. The first multi-material 3D printer was presented in 2006 and used a syringe-based system. This experimental study addresses only two specific additive technologies used in developing the protective UV-C mask (SLS, MJF). It should be also mentioned that the 3D printers that work on the principle of fusible link production, Fused Filament Fabrication (FFF), are currently more affordable for the public. In this case, the FPP2 filter housing and internal and external exhalation valves for the prototype protective half-face mask can be 3D printed out of the Fused Filament Fabrication (FFF) technology. The 3D printer, which works on the Fused Filament Fabrication technology (FFF), can simultaneously print a 3D object using several materials [15]. From the knowledge gained from practice, we can conclude that the primary motivation and goal of the 3D printer researchers was the integration of additive technologies into the electronic industry, aviation, bioengineering, robotics, textile industry and development centers, which was achieved [15]. It should also be noted that the ISO/ASTM 529000:2015 standard categorizes the additive technologies into seven main groups [16].

2.1 Three different PA12 powder materials for the experimental samples

At the beginning of 2020, many protective face shields made of polypropylene were used worldwide. Authors of the manuscript [17] verified that the 3D printable extruded material could produce be recycled and reused for 3D printing. However, this experimental study aims to develop and research materials for a prototype protective half-face mask from polyamide 12 (PA12). Within the experimental measurement of the surface roughness 3 test samples were prepared from three different PA12 powder materials (Table 1) of a rectangle shape of 50 mm x 30 mm x 10 mm.

Each sample was printed with another 3D printer. The first sample was printed out with a printer from SINTERIT company, the second sample was with an EOS printer and the third sample was printed out with an HP printer. The 3D printers worked during printing with the powdered material PA12 according to the specific requirements of additive technology (SLS, MJF) and the manufacturer's recommendations.

Table 1 *List of samples used in the experiment*

Samples	AM - No.1	AM - No.2	AM - No.3
Used additive technology	SLS (5W)	SLS (60W)	MJF
The powder material	PA12 Smooth	PA12 PA 2 200	PA12 MJF

Figure 2 *EinScan - SP 3D scanner*

2.2 Photogrammetry - 3D projection

Three-dimensional scanning brings the best choice for obtaining data from physical objects into a digital 3D model. In the 21st century, it is characteristic of the start of the fourth industrial revolution, which presents these technologies. The manuscript [18] states that the 3D scanning systems can work with or without contact. The 3D scanning technology is currently used in the development and research, design, engineering, healthcare, dentistry, or scanning of parts of the human body, as well as in archaeology. Prototyping has become a certain standard in the field of healthcare especially.

Additive manufacturing is used for production of Orthopedic Prosthetics devices, as well. In [19] the authors described the 3D printing and the application of Orthopedic Prosthetics in an industrial area. An example can be the manuscript [20] in which the authors published research results on foot deformation with bearing conditions to improve the design of diabetic footwear. Last but not be least, the authors of [21] used the 3D scanner EinScan-SP to scan the foot deformities.

In addition, dentistry uses 3D scanning; for example, a manuscript [22] confirmed the suitability of intraoral digital scanners for scanning the entire arch for dental patients. The other significant publications of the authors [23-27] present results from their actual medical practice.

The use of photogrammetry is varied. The mentioned authors used the non-contact and non-destructive 3D laser scanning technology during the research and development. The authors [28] stated more information about the technology of 3D scanning in their manuscript.

Technologies of the 3D scanning are just now used in a wide range of various applications. Additionally, photogrammetry use is in scanning museum archaeological objects [29]. Next, in the area of reverse engineering a 3D scan is used for the mechanism's physical parts that lack documentation or have changed from the original CAD design of the element [30]. Scanned 3D objects can be used in further work in virtual assemblies utilizing the CAD system. The EinScan-SP scanner has a fully automatic mode for larger objects with the support of a tripod.

During the development of the protective UV-C mask benefits of the powerful EinScan-SP 3D scanner were used, Figure 2. EinScan features two scanning modes. The first is Fixed Scan (manual control) and the second is Auto Scan. The fully automatic mode is only suitable for up to 5 kg objects with the support of a tripod. The smaller physical objects need a rotary table. When the rotary table is used, it is possible to scan objects with an accuracy of 0.05 mm. In addition to the fixed scanner placement on the tripod, the scanner, even outside the tripod, creates digital 3D objects. EinScan device is recommended in manual mode for objects heavier than 5 kg, of lengths more than 25 cm and for items with complex geometry. In this case, the object to be scanned is placed on a flat surface and gradually rotated manually. The human body is 3D scanned using this manual mode. The advantage of the EinScan-SP scanner is that it provides a new human face and hair scanning mode that works with an invisible infrared light source. It offers a reliable solution even for dark-colored scanning objects and, last but not the least, has high accuracy. The Ein Scan-SP scanner software also adjusts the data coordinates in the post-processing process, which provides spotless 3D data for subsequent applications [31]. Another advantage is that the scanned 3D objects can be used in further work in virtual assemblies utilizing the CAD system [31].

2.3 Selective laser sintering (SLS)

The selective laser sintering (SLS) is a method that creates physical models through the selective solidification of various fine powders and has received much attention in the clinical field [32]. During the 3D printing, tiny powder particles with 18 to 80 μm are sintered. Selective laser sintering (SLS) ranks among a solid freeform fabrication technique developed

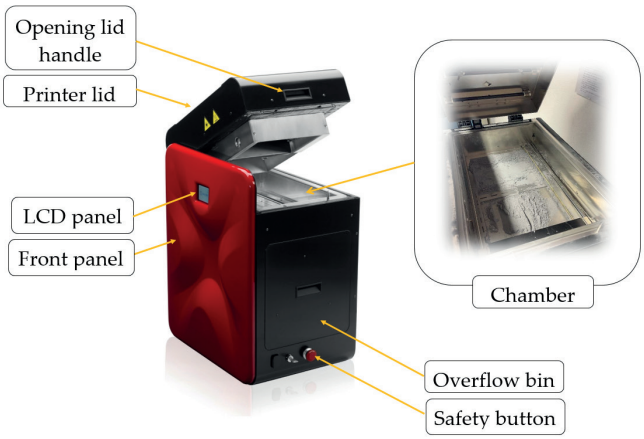

Figure 3 *The 3D printer of the Sinterit Lisa in the laboratory [34]*

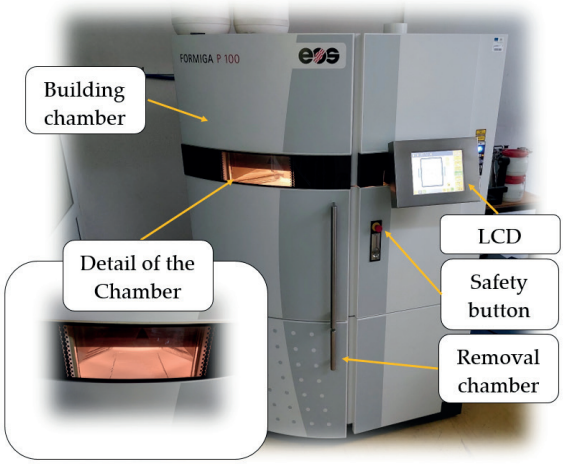

Figure 4 *The 3D printer of the EOS Formiga P100 in the laboratory*

by Deckard for his thesis at the University of Texas, patented in 1989 [32]. The authors of [33] thoroughly addressed the issue of polymers produced using the SLS technology. They developed a transparent production methodology based on research using the desktop printers with selective laser sintering (SLS). The critical aspects described in the manuscript can also apply to developing a protective UV-C half-face mask.

The first used 3D printer Lisa (Figure 3) from Sinterit Lisa, has a laser with a power of 5 - Watts. The working principle of the Lisa 3D printer consists in fusing the powder material with a laser beam. The printer works with the SLS technology, which sinters the powder material layer by layer using a laser emitter. The current market offers several powder materials that apply to Sinterit Lisa. The best known are the PA12 powder material, PA11 and polypropylene (PP) [34].

The Lisa printer can print any shaped object in the printer space. It should be noted that the Sinterit Lisa printer offers the printing of 3D objects without supporting materials, which represents a significant advantage [34]. The Sinterit Lisa can be placed on a worktable thanks to its smaller dimensions, what ultimately brings a practical solution. In general, however, the objects made using the mentioned additive technology (SLS) have a superior surface quality and incomparable mechanical and temperature resistance up to 120 °C. One advantage of the Sinterit Lisa printer is the reuse of unused dust, which is found together with the model in the print cake [34]. The 3D Sinterit Lisa printer can also bake with flex grey powder material - TPU (Thermoplastic Polyurethane Elastomer), which makes it possible to create the 3D prints of high elasticity.

The second 3D printer used, the Formiga P100 from EOS company (Figure 4), uses a 60 - Watt laser to sinter particles of PA12 powder material.

The EOS Formiga P100 printer prints vertical walls of objects with maximum surface quality. For this reason, the printer is ideally suited for small filigree components, precisely like those that make up a protective UV-C face half-mask. The manufacturer states the vertical accuracy at distances of 300 mm ± 0.05 mm. The development of the EOS Formiga P100 printer was primarily aimed for that parameter. Sinterit Lisa (Figure 3) and EOS Formiga P100 (Figure 4)

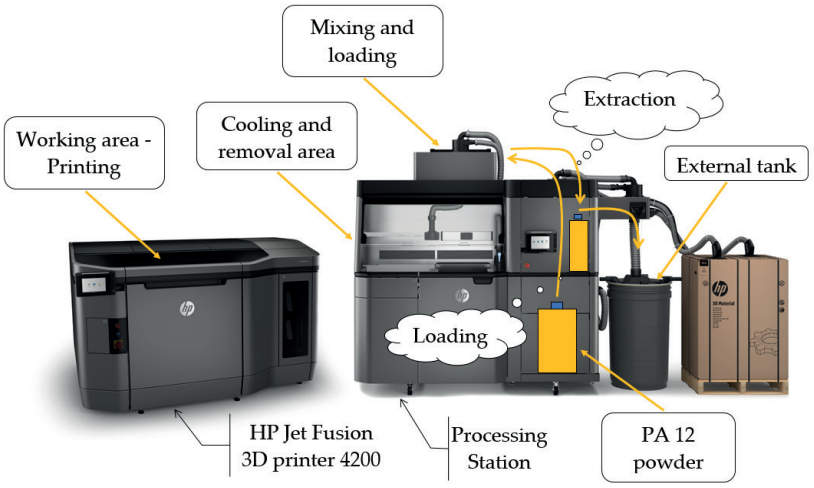

Figure 5 *HP Jet Fusion 3D printer 4200 [35]*

devices offer 3D printing of PA12 using selective laser sintering (SLS). The listed printers differ in dimensions and, above all, sintering performance.

2.4 Multi jet fusion 3D printer

The last 3D printer, used in developing the UV-C protection half-face mask, is the HP Jet Fusion 3D 4200. The device works with Multi-Jet Fusion (MJF) technology. The last sample AM-No. 3, was printed from unique PA 12 powder material, designated for Multi-Jet Fusion sintering technology. The mentioned HP printer can print the PA12 powder material, the polypropylene (PP) and thermoplastic polyurethane (TPU 90A) [35]. After producing three samples from the powder material, visual differences were visible in the surface structure of every experimental sample. Ultimately, the quality of the 3D print depends on the 3D printer technologies. During the development of the protective UV-C face half-mask, emphasis was placed not only on the quality of the surface, which does not let water, viruses and bacteria through the surface of the half-face mask. The EOS Formiga P100 printer produces vertical walls of 3D objects with maximum surface quality.

For this reason, the system is ideally suited for small filigree components, precisely like those that make up a protective UV-C face half-mask. The manufacturer states the vertical accuracy at distances of 300 mm ± 0.05 mm. TThe last sample was made of the PA12 powder material, suitable for multi-jet fusion sintering technology. The research examines several prints' surface quality for the proposed protective half-face mask as a primary goal.

Some medical devices are, at this time, already produced using modern 3D printers with sintering metal powder (SLM) technology. The authors of [36] present experiences with developing medical devices and other applications. In their manuscript, the authors describe attempts to optimize some process properties, such as surface roughness, porosity and mechanical properties of 3D prints. The authors also described the issue in great detail, to understand the existing research gaps. The publication [36] outlines some critical aspects for further development of the technique of selective laser sintering of metal powder, especially in medical applications, which needs consideration. In addition, optimizing process properties, such as surface roughness, porosity and mechanical properties for the 3D prints PA12, printed out with selective laser sintering (SLS) technology, is similarly necessary. Authors of [37] correctly noted one fact. Before achieving more economical production, one must decide on the setup of the 3D printer to economically print parts with good mechanical behavior. They also noted that if the hatch spacing, laser power and scanning speed are selected so that the laser energy density was too high, the powders would burn and the printing process would fail.

2.5 Alicona Infinite Focus G5 and observing 2D and 3D roughness of the samples

The team of researchers defined the essential attributes the protective half-face mask must meet at the beginning of development. The first two important, characteristic primary features that the half-face mask must fulfill are focused on the ideal shape design as well as on the high-quality non-porous material, which is necessary for the correct function of the half-face mask. This second most significant requirement defines the zero penetration of air and liquids through the material's structure of the print-out from PA12 of the powder material. The third condition discusses how the surface of the protective half-face mask will

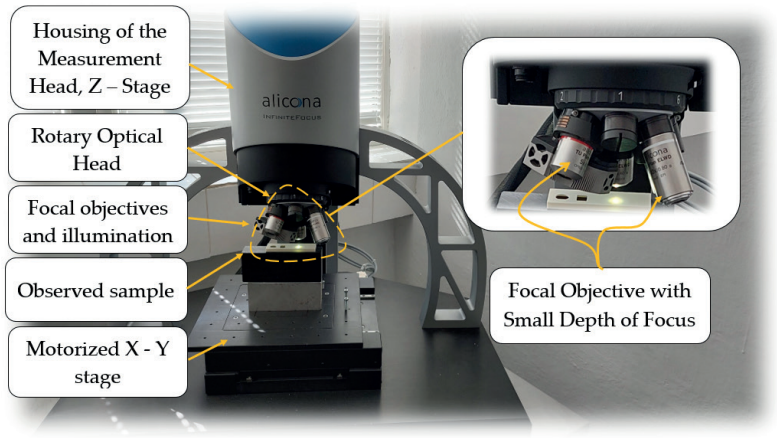

Figure 6 *Alicona Infinite Focus G5*

Figure 7 *3D digital head form-EinScan-SP before digital modification*

Figure 8 *3D digital head form EinScan SP after digital modification*

not be additionally finished after being printed out. It means that the surface structure of the half-face mask should not be enormously rough, but pleasant to the touch after print-out. For this reason, it was necessary to investigate all the samples' roughness, porosity and surface topography. All the samples' surface roughness structures were analyzed using the Alicona Infinite Focus G5 device (Figure 6).

3 Results of the experimental study

The facial features recorded with the 3D EinScan-SP scanner are essential in developing the UV-C protective half-face mask design. The scanned digital model of the head (Figure 7) was subsequently phase modified (Figure 8). The digital model of the human face is used to create the basic parametric model of the protective UV-C face half mask. After printing, the half-face mask should be perfectly sitting on the chin, cheekbones and nose.

The human head's anthropology data was collected using the 3D scanning technology, the so-called photogrammetry-3D projection. The software of the Ein Scan-SP scanner automatically generated a digital file human head, which was subsequently edited by the modeling software Ein Scan-SP scanner. During the scanning, imperfections arose in the digital model in the form of hole shapes. For this reason, using the software Ein Scan the digital model was modified and the holes were filled, smoothed and sharpened. This process aimed to provide the perfect 3D data for the parametric design of the mask in Creo parametric software from PTC company.

3.1 Design of the UV - C half mask

Development of the half-face mask was primarily the parametric 3D model focused, including creating a chamber with an air disinfection system using a UV-C light source. The developers also emphasized the overall appearance and ergonomic shapes of the proposed prototype of the protective half-face mask. In developing the protective UV-C half-face mask the Creo Parametric software was used, with a standard modeling tool and the ISDX (Interactive Surface Design Extension) tool, which allows the modeling of free surfaces (Figure 9).

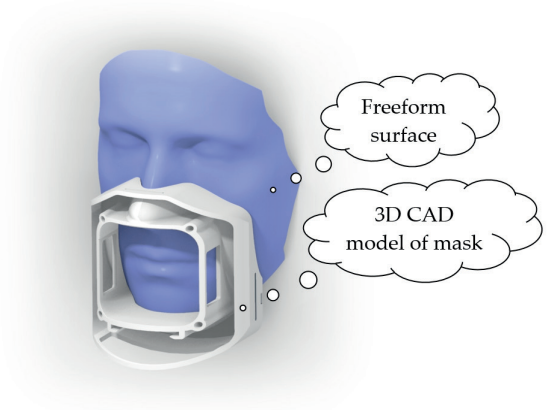

Figure 9 *Enhanced Interactive Head Surface (ISDE)*

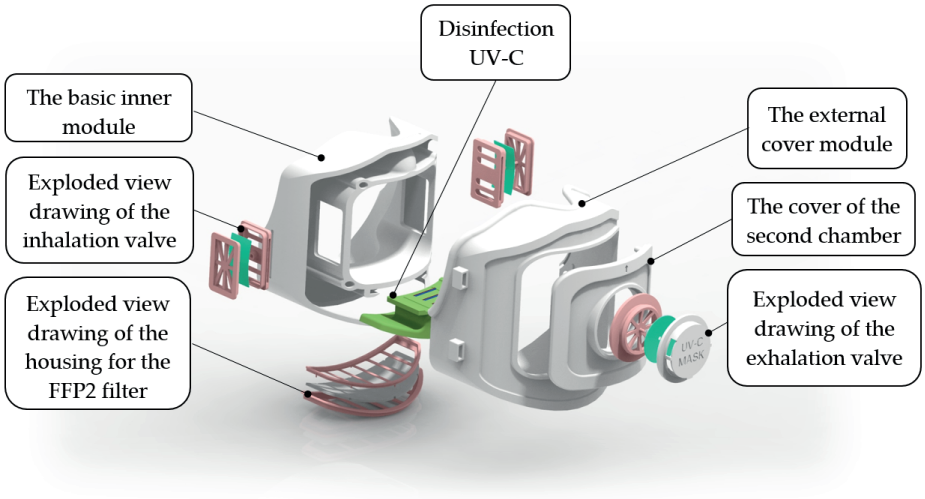

Figure 10 *Protective UV-C half-face mask in the exploded view*

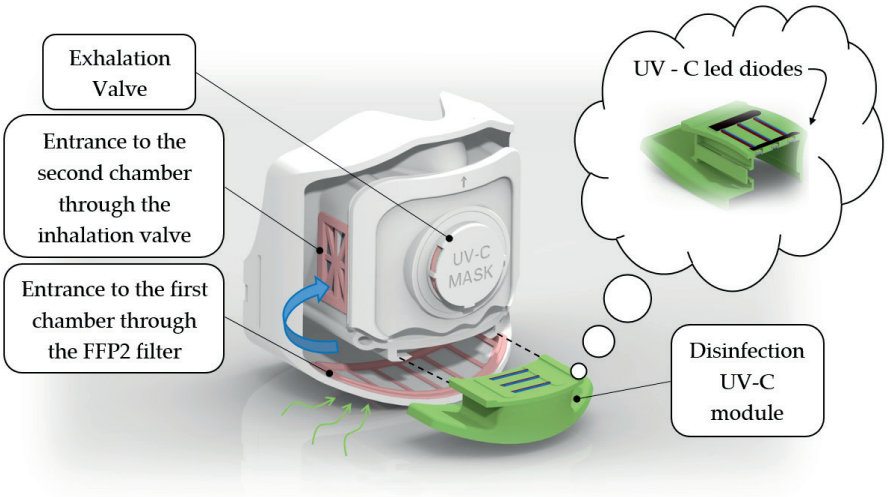

Figure 11 *Construction of the UV-C half-face mask*

In the current era of the 21st century, software tools already handle the demanding requirements of high-quality free characters (class A surfaces), similar to the modeling of structural components using the power of parametric modeling.

The prototype development of the protective UV-C half-face mask used the experience of the researchers from the Rapid Prototyping laboratory. During the development of the mask, the results and experiences of prototyping from publication [38] were applied, as well.

Figure 12 *Inside part of protective UV-C half-face mask*

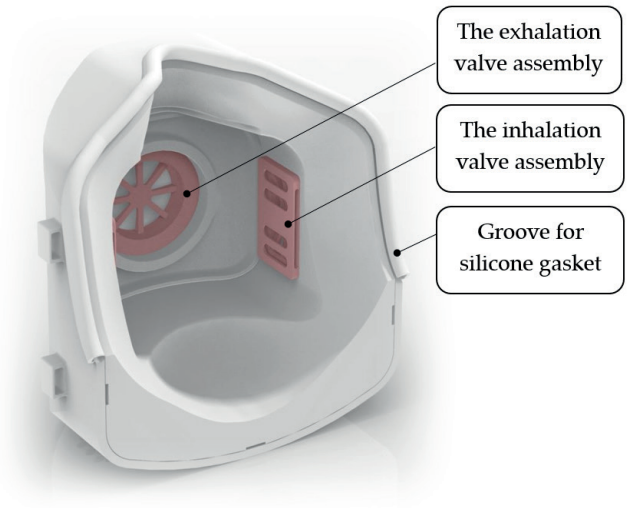

Figure 13 *Inside part of protective UV-C half-face mask*

The parametric 3D model of the protective UV-C half-face mask consists of seven parts. The module for the internal valve the exhalation valve and the FFP2 filter housing comprises two separate parts and the rubber valve together form an assembly. The illustration below shows a parametric 3D prototype of a protective UV-C half-face mask, Figure 10.

The protective half-face mask's working principal rests in disinfecting the air-inhaled using the UV-C light. The inner part of the protective half-face mask has two separate chambers. The first chamber is named the "disinfection module" and forms a separately removable part of the mask. Inhaled air enters the disinfection module with UV-C LED through the FFP2 filter on the bottom of the mask. The air stream slows down in the disinfection module as it passes through the labyrinth-shaped holes. In this case, the slower-flowing air is cleaned effectively of pathogens with UV-C light. The space of the second chamber accumulates the disinfected air, which the person subsequently breathes (Figure 11).

The inside valve design ensures that the airflow direction is always from the accumulation chamber to the other section, never in the opposite direction. During inhaling, the person breathes disinfected air, passing through the two side valves into the second chamber. During exhalation, the consumed air is enriched with CO_2 and exhaled through the exhalation valve into the surrounding space. The external exhalation valve works on a similar principle. However, the air fluxed is the opposite, as in the case of the two internal valves. The air flows from the exhalation valve only to the surrounding area, never back inside.

The protective half-mask is removable for more accessible cleaning of all corners and inaccessible crevices. An outer part of the mask covers the space where the disinfected air is maintained. The figure below illustrates four slots integrated into the outer part of the mask, respectively, the outer cover (Figure 12).

The 3D model of the prototype protective half-face mask contains two side valves on both the right-hand

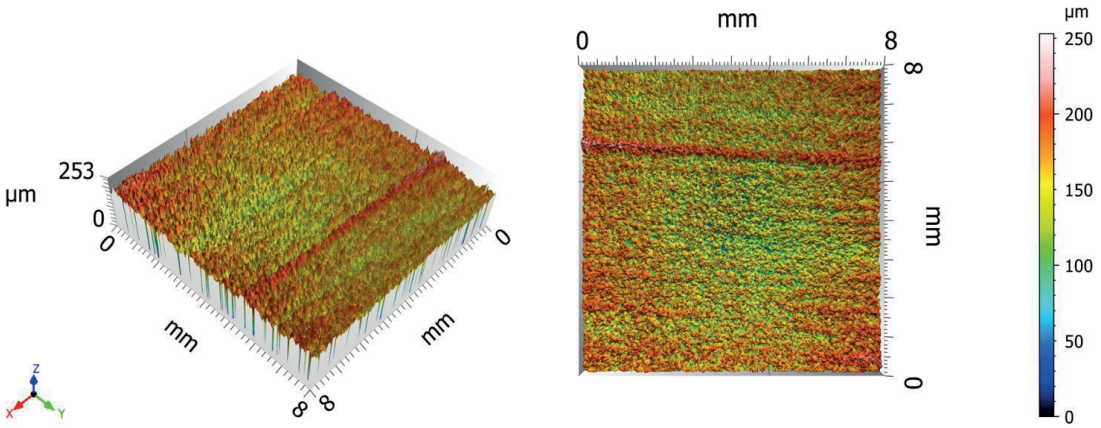

Figure 14 *Primary surface PA12 - Smooth - Selective laser sintering (SLS)*

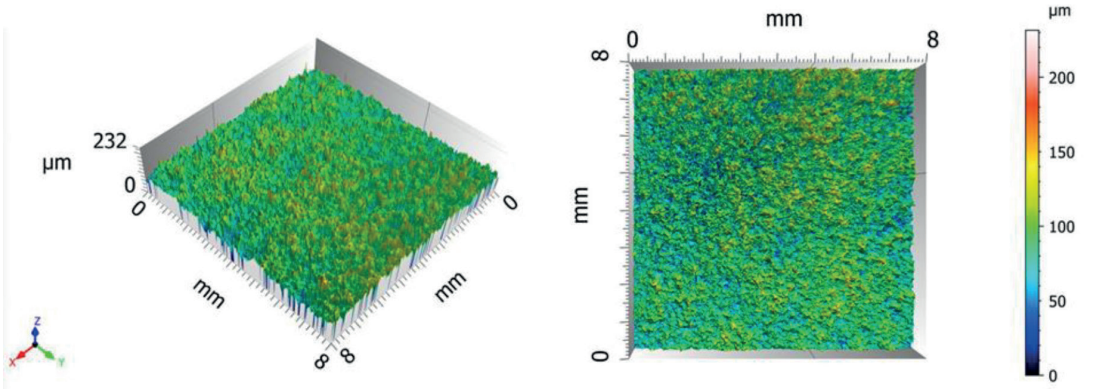

Figure 15 *Primary surface PA12 - PA 2 200 - Selective Laser Sintering (SLS)*

and left-hand sides. However, one valve is visible on the back side of the protective half-face mask (Figure 13). The front round valve exhales consumed air. Both inside valves use musk rubber, ensuring air penetration into and out of the chambers. The outer cover is equipped by a groove for a silicone gasket, which is visible on the back side of the outer surface of the mask.

3.2 Observation of the surface topography of PA12 with Alicona infinite Focus G5

The last stage of experimental research was focused on the samples' surface topography investigation. The 3D graphs show the primary surface of samples in perfect natural resolution and clarity. The display of colors is authentic and at a high micro level. The results of investigation follow ISO 16610 - 61 standards. Additionally, the roughness profile is shown in a 2D diagram with a complete RA surface roughness analysis. Figure 14 shows the primary surface of sample AM - No.1 (PA12 - Smooth) at 100 times magnification. The unevenness of the primary surface ranged from 350 to 100 µm.

Figure 15 presents the primary surface of sample AM - No.2, made of powder material PA12 - PA 2 200 at 100 times magnification. The sample showed more pores and minor irregularities in the surface structure. In addition, the unevenness of the primary surface ranged from 100 to 240 µm. The second sample, AM - No.2, was printed by selective laser sintering technology on the printer EOS Formiga P100.

The last sample, AM - No.3, was prepared by additive Multi-Jet Fusion (MJF) technology. At 100 - fold magnification regularly repeating waves are seen on the structure of the surface that arise after applying the powder material (Figure 16). The unevenness of the primary surface ranges from 120 to 180 µm.

The authors of [39] presented research on the surface roughness profile for both parallel and perpendicular orientations of 3D-printed polymers. They concluded that the similar direction shows a consistent periodicity for the surface topography with peak height. However, at perpendicular orientation, the profile shows different peak height values for the scan lengths with a reasonably consistent peak periodicity between the consecutive peaks [39]. The authors of [40] presented the surface roughness of the manufactured parts of the Lisa 3D printer using the Focus Variation (FV) technology. The authors described the experimental investigation of the surface roughness of three samples from PA12. The experimental investigation occurred

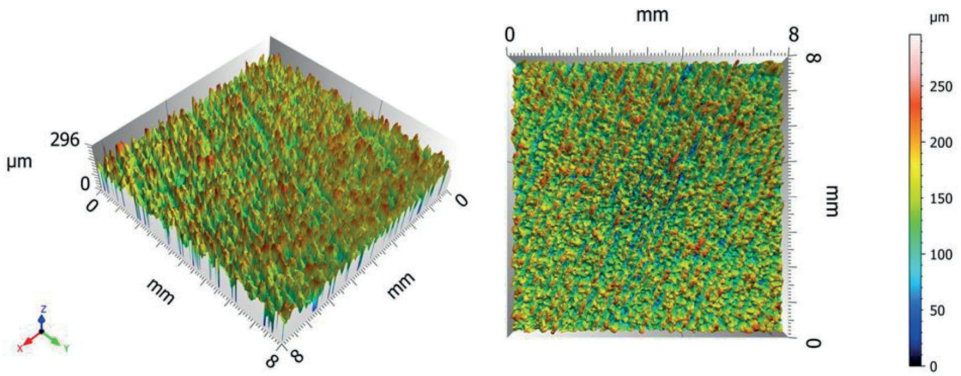

Figure 16 *Primary surface PA12 - MJF - Multi - Jet Fusion (MJF)*

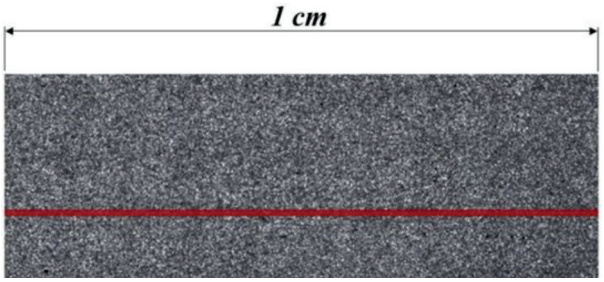

Figure 17 *PA12 Smooth - 2D surface roughness measurement path*

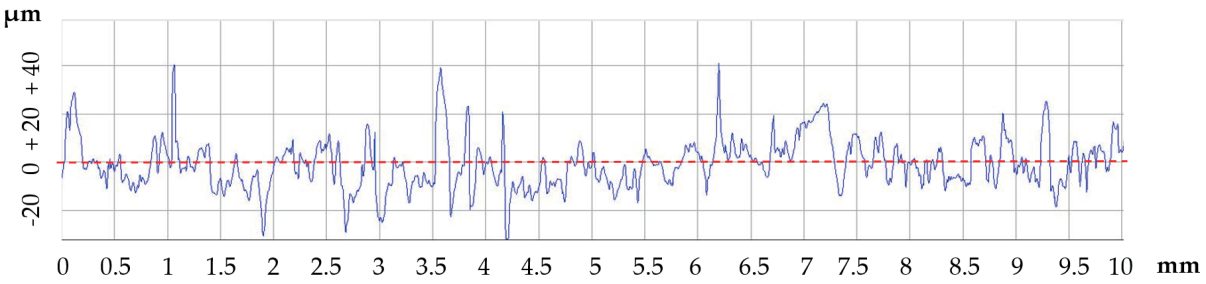

Figure 18 *Diagram of PA12 Smooth profile roughness measurement - Sinterit Lisa*

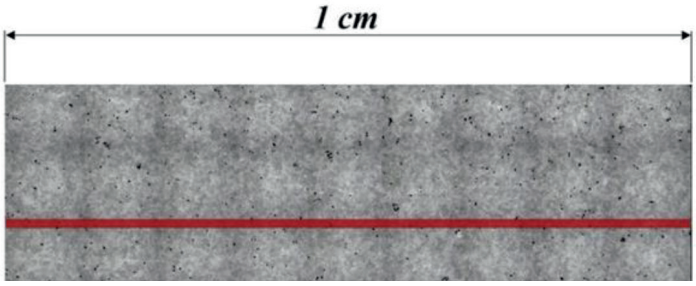

Figure 19 *PA12 Smooth - 2D surface roughness measurement path*

in the certified measurement laboratory, where they investigated the 2D, as well as the 3D surface roughness of the three samples above. The measurement of surface roughness took place with the help of the Alicona Infinite Focus G5 device. The measuring device used an optical sensor IF Sensor C100 G1 to extract the primary surface. During the experimental investigation of the 2D roughness on the sample's surface, 50 roughness profiles per 1 cm length were pulled. The diagrams show the graphic course of roughness results with the worst surface parameters in terms of surface functionality. The red line on each sample (Figures 17-21) represents 1 cm of the length and location of the 2D roughness measurement. During the test, the parameters of the 2D surface roughness (Figures 18-22) were measured. These parameters were the average roughness of the profile (Ra), root mean square roughness (R_q), the mean height of the roughness profile from peak to valley (Rz), maximum roughness profile valley height (R_v) and roughness profile distortion (R_{sk}).

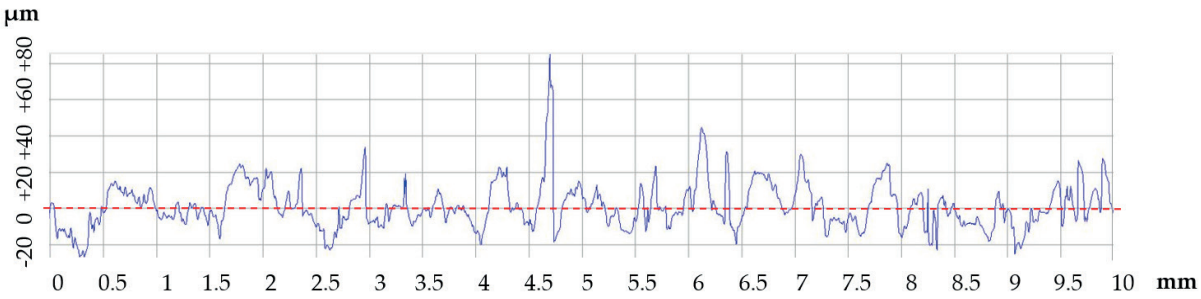

Figure 20 *Diagram of PA 2 200 profile roughness measurement - EOS Formiga*

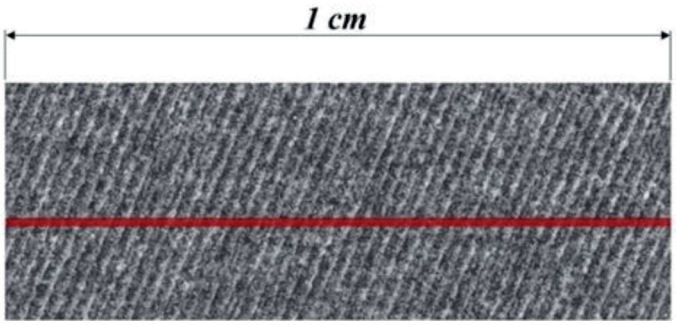

Figure 21 *PA12 Smooth - 2D surface roughness measurement path*

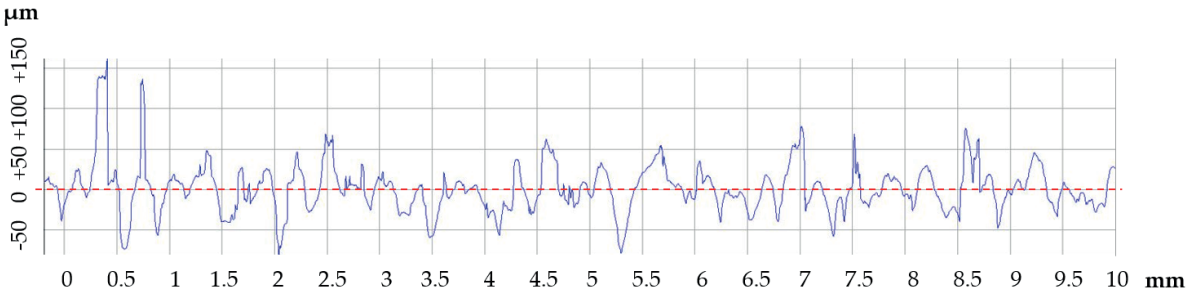

Figure 22 *Diagram measuring the roughness of the PA12 profile - MJF - HP Jet Fusion 3D 4200*

Table 2 *2D surface roughness parameters of all samples*

Samples	R_a (µm)	R_q (µm)	R_z (µm)	R_v (µm)	R_{sk} (µm)	R_v/R_z (µm)
AM - No.1	7.656	10.498	59.421	32.194	0.959	0.541
AM - No.2	9.185	12.499	66.363	28.714	1.430	0.432
AM - No.3	21.200	30.045	157.093	81.992	1.245	0.521

The R_v/R_z ratio is the most important, indicating whether depressions or elevations predominate on the sample's surface. If depressions prevail, cracks may appear in the structure of the polyamide sample. However, in the case of cyclic stress, the split can occur after some time. Bacteria and viruses can accumulate in cracks, which is undesirable for protective half-face masks with a UV-C light source. The acceptable value of the R_v/R_z ratio is in the interval from 0 to 0.55. Ultimately, this finding stems from the long-term research experience of researchers. The results of all investigated parameters are given in Table 2.

From the measured results it is clear that the R_{sk} parameter came out in positive numbers for on all the examined samples. That means that protrusions are predominantly present the surface of each sample. However, when the value R_{sk} of is negative, the sample's surface is dominated by holes. The R_v/R_z ratio is at the limit of the permissible value of 0.55 for all the samples. The 3D surface roughness was investigated in the last phase of the experiment. When evaluating the surface's topography, the nesting index is fixed to 8 mm. In addition, the evaluation was to use the Gaussian filter. The first sample represents the 3D surface of sample AM - No. 1 (Figure 23). The second sample represents the 3D surface of sample AM - No. 2 (Figure 24).

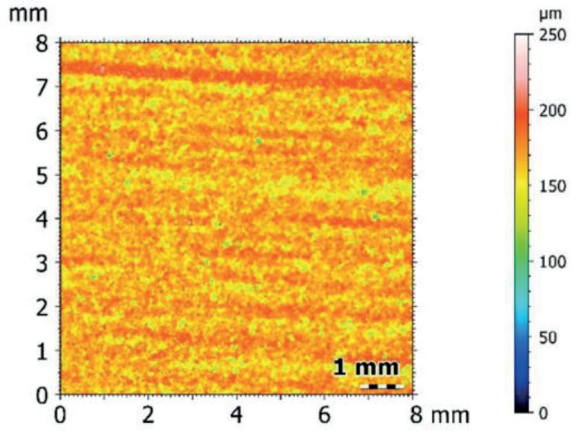

Figure 23 *The 3D roughness PA12 – Smooth*

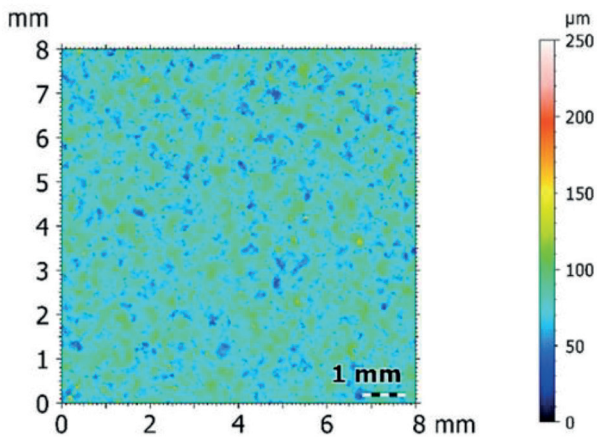

Figure 24 *The 3D surface roughness PA12 – 2200*

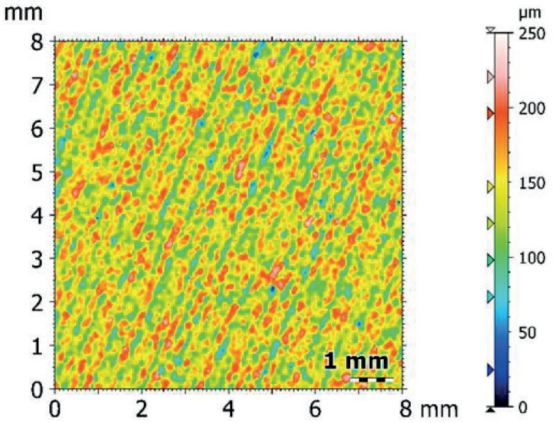

Figure 25 *The 3D surface roughness of PA12 – MJF*

The last sample represents the 3D surface of sample AM - No. 3. The sample is printed-out from PA12 - MJF powder material (Figure 25). During the measurement of 3D roughness, a Gaussian filter (FALG) was applied by the ISO 16610 - 61 standard on all the samples.

4 Discussions

Manuscript [41] listed that the global pandemic that has affected humanity has contributed to the breakdown of traditional supply chains responsible for providing personal protective equipment for health and social staffers.

The researchers' strategy was to mitigate the impact of infectious diseases on the world's population. The researchers of this experimental study decided to contribute with their prototyping experience and proposed a protective UV-C half-face mask.

The protective half-face mask can be printed out on a 3D printer that works with SLM or MJF technology, based on a digital parametric model, in any corner of the world, where the technical means are available. The main idea of this project was to immediately use the created digital mask data. Another part of the research and development was preparing a chamber for disinfecting the inhaled air with a source of UV-C light and preparing the section for breathing disinfected air. Some publications [42-43] state that the ideal wavelength band of UV-C light for the air disinfection, which does not harm human health is the band of wavelengths from 220 to 222 nm. In addition, several publications mention that UV-C light with wavelength band UV from 220 to 222 nm should not produce ozone (O_3) and using UV with said wavelength is biocompatible. Therefore, this claim will continue to be explored and verified. However, the authors of [43] state that further evaluation and testing of the safety and efficacy of the band of wavelengths from 220 to 222 nm UV-C light is needed. Therefore, the research will be extended to clinical evaluation and testing of the wavelength band UV from 220 to 222 nm in the future and its impact on the human health in prolonged use. The project will also focus on other additive technologies and materials suitable for such protective masks. Ultimately, additive technology allows production of parts with complex

designs, with certain limitations depending on the specific additive technology [44-45]. Several researchers dealt with polyamide materials listed in this manuscript within development. The researchers also focus on UV-C portable disinfection boxes for small objects, such as a set of keys, a mobile phone, etc. A team of researchers is also considering developing a device for disinfecting factories' production areas by using a UV-C module mounted on an automated guided vehicle (AGV) cover of the body.

5 Conclusions

The developers used the advantages of the 3D scanning while developing the protective UV-C half-face mask, since in development of a protective half-face mask technology of non-contact and non - destructive 3D laser scanning, details of a human head was needed. As already mentioned at the beginning of the experimental study, as a part of the development of the prototype of the protective UV-C half-face mask, three samples were prepared, which consisted of the PA 12 powder material. However, the final sintering of the PA12 powder material took place on the three 3D printers with different sintering technologies. At the first glance, the difference in the surface structure is easily visible in all samples. It is essential to mention that any additive technology influences the surface roughness of components with PA12 in a certain way. The right choice of a suitable PA12 powder material for a protective half mask is also necessary due to the roughness and porosity of the PA12 material. The research also showed significant differences in surface porosity in all the investigated samples. The first sample, AM - No.1, produced by selective laser sintering of PA12 - Smooth powder material, is biocompatible. Sample AM - No.1 has a smooth surface and is pleasant to the touch. The surface 2D roughness results are the proof and the 3D diagram (Figure 18) proves it, as well. This sample has the minimum number of pores in the structure surface. The second sample of AM - No.2, produced by the EOS Formiga P100 printer, has visible pores in its surface structure that, when enlarged, resembled a sieve. Evidence can be black dots in the 2D diagram (Figure 20), which present holes. The blue to black spots are visible on the chart of the 3D roughness surface of the second sample. Chemical surface protections for technical plastics from practice are known. However, applying a chemical surface treatment to the printed parts of the PA12 material and thus filling a large number of pores is impossible since this protective half-mask is for biocompatible use. The EOS Formiga P100 printer works with selective laser sintering (SLS) technology, similar to the SINTERIT Lisa printer. It is essential to note that the authors of [46] stated that PA 2 200 is biocompatible.

In the case of MJF technology, the sample surface quality (AM - No.3) is, at the first glance, reasonable, it has fewer pores and no additional surface treatment is required. However, the sample made by Multi-Jet Fusion (MJF) technology showed the highest surface roughness value of all three examined samples. The texture in place of the sample's surface resembled a wave shape and rougher. Compared to all the analyzed samples, the last piece, AM - No.3, has a distinct surface structure, which can also be seen at the macro level.

The summary of the experimental investigation of the surface roughness:

- Regarding the surface structure of samples and print quality, PA12 smooth or PA12 MJF material is recommended for the protective UV-C half-face mask.
- Roughness of the PA12 Smoot has a value of Ra 7.656 μm.
- Roughness of the PA12 2200 has a value of Ra 9.185 μm.
- Roughness of the PA12 MJF has a value of Ra 21.200 μm.
- Continue clinical research and testing of the mask, especially the impact of UV-C light at a wavelength of 220 *nm* on human health.

The protecting UV-C half-face mask will find application mainly in medical facilities and public service (fire and police forces etc.). The advantage of the protective UV-C half-face mask is the possibility of repeated use. The use time is limited to one battery charge because the battery provides an electricity source for the UV-C led light. The FFP2 protective filter placed into the mask protects human health for more than four hours. The FFP2 filter is also advisable to replace after each use. In conclusion, it is necessary to appreciate that the collaboration between the 3D printing community and the healthcare system has helped in providing innovative solutions to combat the crisis.

Acknowledgment

This article was funded by the University of Zilina project 313011ASY4 "Strategic implementation of additive technologies to strengthen the intervention capacities of emergencies caused by the COVID - 19 pandemic."

Conflicts of interest

The authors declare that they have no known competing financial interests or personal relationships that could have appeared to influence the work reported in this paper.

References

[1] ARMENTANO, I., BARBANERA, M., CAROTA, E., CROGNALE, S., MARCONI, M., ROSSI, S., RUBINO, G., SCUNGIO, M., TABORRI, J., CALABRO, G. Polymer materials for respiratory protection: processing, end use and testing methods. *ACS Applied Polymer Materials* [online]. 2011, **3**(2), p. 531-548. eISSN 2637-6105. Available from: https://doi.org/10.1021/acsapm.0c01151

[2] WESEMANN, C., PIERALLI, S., FRETWURST, T., NOLD, J., NELSON, K., SCHMELZEISEN, R., HELLWIG, E., SPIES, B. CH. 2 3-D printed protective equipment during COVID-19 pandemic. *Materials* [online]. 2020, **13**(8), 1997. eISSN 1996-1944. Available from: https://doi.org/10.3390/ma13081997

[3] ZUNIGA, J. M., CORTES, A. The role of additive manufacturing and antimicrobial polymers in the COVID-19 pandemic. *Expert Review of Medical Devices* [online]. 2020, **17**(6), p. 477-481. ISSN 1743-4440, eISSN 1745-2422. Available from: https://doi.org/10.1080/17434440.2020.1756771

[4] COOK, T. M. Personal protective equipment during the coronavirus disease (COVID) 2019 pandemic - a narrative review. *Anaesthesia* [online]. 2020, **75**(7), p. 920-927. eISSN 1365-2044. Available from: https://doi.org/10.1111/anae.15071

[5] NOURAZARAN, M., YOUSEFI, R., MOOSAVI-MOVAHEDI, A. A. Effects of vitamin D in fighting COVID-19 disease. *Iranian Journal of Nutrition Sciences and Food Technology* [online]. 2022, **16**(4), p. 121-130. ISSN 1735-7756, eISSN 2252-0694. Available from: http://nsft.sbmu.ac.ir/article-1-3294-en.html

[6] VARANGES, V., CAGLAR, B., LEBAUPIN, Y., BATT, T., WEIDONG, H., WANG, J., ROSSI, R. M., RICHNER, G., DELALOYE, J.-R., MICHAUD, V. On the durability of surgical masks after simulated handling and wear. *Scientific Report s*[online]. 2022, **12**(1), 4938. eISSN 2045-2322. Available from: https://doi.org/10.1038/s41598-022-09068-1

[7] US Department of Labor [online] [accessed 2021-02-01]. Available from: https://www.osha.gov/news/newsreleases/trade/08032021

[8] ZHUANG, Z. Head-and-face anthropometric survey of U.S. respirator users [online]. Final report. Available from: https://nap.nationalacademies.org/resource/11815/Anthrotech_report.pdf

[9] ZHUANG, Z., BRADTMILLER, B. Head-and-face anthropometric survey of U.S. respirator users. *Journal of Occupational and Environmental Hygiene* [online]. 2005 **2**(11), p. 567-576. ISSN 1545-9624, eISSN 1545-9632. Available from: https://doi.org/10.1080/15459620500324727

[10] SWENNEN, GWEN, R. J., LIES, P., HAERS, P. E. Custom-made 3D-printed face masks in case of pandemic crisis situations with a lack of commercially available FFP2/3 masks. *International Journal of Oral and Maxillofacial Surgery* [online]. 2020, **49**(5), p. 673-677. ISSN 0901-5027, eISSN 1399-0020. Available from: https://doi.org/10.1016/j.ijom.2020.03.015

[11] PIOMBINO, P., COMMITTERI, U., NORINO, G., VAIRA, L. A., TROISE, S., MAGLITTO, F., MARINIELLO, D., DE RIU, G., CALIFANO, L. Facing covid-19 pandemic: development of custom-made face mask with rapid prototyping system. *Journal of Infection in Developing Countries* [online]. 2021, **15**(1), p. 51-57. ISSN 972-2680. Available from: https://doi.org/10.3855/jidc.13384

[12] PRABHU, R., BERTHEL, J. T., MASIA, J. S., MEISEL, N. A., SIMPSON, T. W. Rapid response! Investigating the effects of problem definition on the characteristics of additively manufactured solutions for COVID-19. *Journal of Mechanical Design Transactions of the ASME* [online]. 2022, **144**(5), 054502. ISSN 1050-0472, eISSN 1528-9001. Available from: https://doi.org/10.1115/1.4052970

[13] KOHAR, R., MADAJ, R., SASIK, R., GAJDAC, I. Rapid prototyping technologies/Rapid prototyping technologie (in Slovak). 1. ed. Zilina, Slovakia: EDIS ZU, 2018. ISBN 978-80-554-1519-2.

[14] KOHAR, R., STOPKA, M., WEIS, P., SPISAK, P., STEININGER, J. Modular 3D printer concept. *IOP Conference Series: Materials Science and Engineering* [online] 2018, **393**, 012092. ISSN 1757-8981, eISSN 1757-899X. Available from: https://doi.org/10.1088/1757-899X/393/1/012092

[15] MEHRPOUYA, M., TUMA, D., VANEKER, T., AFRASIABI, M., BAMBACH, M. AND GIBSON, I. Multimaterial powder bed fusion techniques. *Rapid Prototyping Journal* [online]. 2022, **28**(11), p. 1-19. eISSN 1355-2546. Available from: https://doi.org/10.1108/RPJ-01-2022-0014

[16] WOHLERS, T., CAFFREY, T. Wohlers report 2014: 3D printing and additive manufacturing state of the industry annual worldwide progress report. Fort Collins, Col.: Wohlers Associates, 2014.

[17] BATTEGAZZORE, D., CRAVERO, F., BERNAGOZZI, G., FRACHE, A. Designing a 3D printable polypropylene-based material from after use recycled disposable masks. *Materials Today Communications* [online]. 2022, **32**, 103997. eISSN 2352-4928. Available from: https://doi.org/10.1016/j.mtcomm.2022.103997

[18] ABDELMOMEN, M., DENGIZ, F.O., TAMRE, M. Survey on 3D technologies: case study on 3D scanning processing and printing with a model. In: International Conference on Research and Education in Mechatronics REM: proceedings [online]. 2020. ISBN 978-1-7281-6225-6, eISBN 978-1-7281-6224-9. Available from: https://doi.org/10.1109/REM49740.2020.9313881

[19] GOLOVIN, M. A, MARUSIN, N. V., GOLUBEVA, Y. B. Use of 3D printing in the orthopedic prosthetics industry. *Biomedical Engineering*, **52**(2), 2018, p. 100-105. ISSN 0006-3398, eISSN 1573-8256. Available from: https://doi.org/10.1007/s10527-018-9792-1

[20] ZHANG, L., YICK, K. L., LI, P. L., YIP, J., NG, S. P. Foot deformation analysis with different load-bearing conditions to enhance diabetic footwear designs. *PloS ONE* [online]. 2022, **17**(3), e0264233. eISSN 1932-6203. Available from: https://doi.org/10.1371/journal.pone.0264233

[21] KARTINI, W., IKHSAN, M., ISMAIL, R., JAMARI, J., BAYUSENO, A. P. Use of 3D scanner and photogrammetry method for scanning foot deformities: CAD data analysis of morphology and shape of geometry. *ARPN Journal of Engineering and Applied Sciences*. 2020, **15**(13), p. 1419-1425. ISSN 1819-6608.

[22] NULTY, A. B. A comparison of full arch trueness and precision of nine intra - oral digital scanners and four lab digital scanners. *Destiny Journal* [online]. 2021, **9**(7), 75. eISSN 2304-6767. Available from: https://doi.org/10.3390/dj9070075

[23] TAPPA, K., JAMMALAMADAKA, U. Novel biomaterials used in medical 3D printing techniques. *Journal of Functional Biomaterials* [online]. 2018, **9**(1), 17. eISSN 2079-4983. Available from: https://doi.org/10.3390/jfb9010017

[24] MUSSI, E., SERVI, M., VOLPE, Y., FACCHINI, F. A simple interactive tool for the CAD modelling of surgical guides for autologous ear reconstruction. *Computer-Aided Design and Applications* [online]. 2023 **20**(1), p. 109-118. ISSN 1686-4360. Available from: https://doi.org/10.14733/cadaps.2023.109-118

[25] KHYATI, D., ZAHERI, M., GOMES, G. V. Superhydrophilic 3D-printed scaffolds using conjugated bioresorbable nanocomposites for enhanced bone regeneration. *Chemical Engineering Journal* [online]. 2022, **445**, 136639. ISSN 1385-8947, eISSN 1873-3212. Available from: https://doi.org/10.1016/j.cej.2022.136639

[26] HABIB, A. A. I., SHEIKH, N. A. 3D printing review in numerous applications for dentistry. *Journal of The Institution of Engineers (India): Series C* [online]. 2022, **103**(4), p. 991-1000. ISSN 2250-0545, eISSN 2250-0553. Available from: https://doi.org/10.1007/s40032-022-00810-2

[27] CRISTACHE, C. M., GROSU, R. A. C., CRISTACHE, G., DIDILESCU, A. C., TOTU, E. E. Additive manufacturing and synthetic polymers for bone reconstruction in the maxillofacial region. *Plastic materials / Materiale Plastice* [online]. 2018, **55**, p. 555-562. ISSN 0025-5289, eISSN 2668-8220. Available from: https://doi.org/10.37358/mp.18.4.5073

[28] TREBUNA, P., TROJAN, J., MIZERAK, M., KLIMENT, M. 3D scanning - Technology and Reconstruction/3D skenovanie - technologia a rekonstrukcia (in Slovak). In: 23th International Scientific Conference Trends and Innovative Approaches in Business Processes: proceedings. Vol. 21. 2018. ISBN 978-80-553-3210-9.

[29] KHRIES, H. M. Photogrammetry versus 3D scanner: producing 3D models of museums' artifacts. *Collection and Curation* [online]. 2021, **40**(4), p. 153-157. ISSN 2514-9326. Available from: https://doi.org/10.1108/CC-06-2020-0021

[30] KUS, A. Implementation of 3D optical scanning technology for automotive applications. *Sensors* [online]. 2009, **9**(3), p. 1967-1979. eISSN 1424-8220. Available from: https://doi.org/10.3390/s90301967

[31] Sinterit Lisa user manual - Sinterit Sp.z o.o. [online] [accessed 2021-02-01]. Available from: https://sinterit.com/wp-content/uploads/2021/12/LISA-1.5_full-user-manual_1.5.pdf

[32] MAZZOLI, A. Selective laser sintering in biomedical engineering. *Medical and Biological Engineering and Computing* [online]. 2013, **51**(3), p. 245-256. ISSN 0140-0118, eISSN 1741-0444. Available from: https://link.springer.com/article/10.1007/s11517-012-1001-x

[33] CHAVEZ, L. A., IBAVE, P., HASSAN, M. S., HALL-SANCHEZ, S. E., BILLAH, K. M. M., LEYVA, A., MARQUEZ, C., ESPALIN, D., TORRES, S., ROBISON, T., LIN, Y. Low - temperature selective laser sintering 3D printing of PEEK - nylon blends: impact of thermal post-processing on mechanical properties and thermal stability. *Journal of Applied Polymer Science* [online]. 2022, **139**(23), 52290. eISSN 1097-4628. Available from: https://doi.org/10.1002/app.52290

[34] Lisa SLS 3D printer - Sinterit Sp.z o.o. [online] [accessed 2021-02-01]. Available from: https://sinterit.com/3dprinters/lisa/

[35] HP Multi Jet Fusion technology - HP Development Company [online] [accessed 2023-01-15]. Available from: https://h20195.www2.hp.com/v2/GetDocument.aspx?docname=4AA5-5472ENW

[36] LA FE-PERDOMO, I., RAMOS-GREZ, J. A., BERUVIDES, G., MUJICA, R. A. Selective laser melting: lessons from medical devices industry and other applications. *Rapid Prototyping Journal* [online]. 2021, **27**(10), p.1801-1830. ISSN 1355-2546. Available from: https://doi.org/10.1108/RPJ-07-2020-0151

[37] RAZAVIYE, M. K., TAFTI, R. A., KHAJEHMOHAMMADI, M. An investigation on mechanical properties of PA12 parts produced by a SLS 3D printer: An experimental approach. *CIRP Journal of Manufacturing Science and Technology* [online]. 2022, **38**, p. 760-768. ISSN 1755-5817, eISSN 1878-0016. Available from: https://doi.org/10.1016/j.cirpj.2022.06.016

[38] MADAJ, R., KOHAR, R. Additive Technologies/Aditivne technologie (in Slovak). 1 ed. Zilina, Slovakia: EDIS ZU, 2020. ISBN 978-80-554-1685-4.

[39] DANGNAN, F., ESPEJO, C., LISKIEWICZ, T., GESTER, M., NEVILLE, A. Friction and wear of additive manufactured polymers in dry contact. *Journal of Manufacturing Processes* [online]. 2020, **59**, p. 238-247. ISSN 1526-6125, eISSN 2212-4616. Available from: https://doi.org/10.1016/j.jmapro.2020.09.051

[40] PETZOLD, S., KLETT, J., SCHAUER, A., OSSWALD, T. A. Surface roughness of polyamide 12 parts manufactured using selective laser sintering. *Polymer Testing* [online]. 2019, **80**, 106094. ISSN 0142-9418, eISSN 1873-2348. Available from: https://doi.org/10.1016/j.polymertesting.2019.106094

[41] IBRAHIM, N., JOVIC, T., JESSOP, Z. M., WHITAKER, I. S. Innovation in a time of crisis: a systematic review of three - dimensional printing in the COVID-19 pandemic. *3D Printing and Additive Manufacturing* [online]. 2021, **8**(3), p. 201-215. ISSN 2329-7662, eISSN 2329-7670. Available from: https://doi.org/10.1089/3dp.2020.0258

[42] FUKUI, T., NIIKURA, T., ODA, T., KUMABE, Y., OHASHI, H., SASAKI, M., IGARASHI, T., KUNISADA, M., YAMANO, N., OE, K., MATSUMOTO, T., MATSUSHITA, T., HAYASHI, S., NISHIGORI, CH., KURODA, R. Exploratory clinical trial on the safety and bactericidal effect of 222-nm ultraviolet C irradiation in healthy humans. *PloS ONE* [online]. 2020, **15**(8), e0235948. eISSN 1932-6203. Available from: https://doi.org/10.1371/journal.pone.0235948

[43] KITAGAWA, H., NOMURA, T., NAZMUL, T., OMORI, K., SHIGEMOTO, N., SAKAGUCHI, T., OHGE, H. Effectiveness of 222-nm ultraviolet light on disinfecting SARS-CoV-2 surface contamination. *American Journal of Infection Control* [online]. 2021, **49**(3), p. 299-301. ISSN 0196-6553, eISSN 1527-3296. Available from: https://doi.org/10.1016/j.ajic.2020.08.022

[44] NAJMON, J. C., RAEISI, S., TOVAR, A. 2-Review of additive manufacturing technologies and applications in the aerospace industry. In: *Additive Manufacturing for the Aerospace Industry* [online]. FROES, F., BOYER, R. (Eds.). Elsevier Inc. All, 2019. ISBN 978-0-12-814062-8, p. 7-31. Available from: https://doi.org/10.1016/B978-0-12-814062-8.00002-9

[45] LUPONE, F., PADOVANO, E., CASAMENTO, F., BADINI, C. Process phenomena and material properties in selective laser sintering of polymers: a review. *Materials* [online]. 2022, **15**(1), 183. eISSN 1996-1944. Available from: https://doi.org/10.3390/ma15010183

[46] STOIA, D. I., VIGARU, C., OPRIS, C., VASILESCU, M. Properties and medical applications of biocompatible polyamide in additive manufacturing. *Plastic materials / Materiale Plastice* [online]. 2021, **58**(1), p. 113-120. ISSN 0025-5289, eISSN 2668-8220. Available from: https://doi.org/10.37358/MP.21.1.5451